International Journal of Innovative Research and Advanced Studies (IJIRAS)
Volume 4 Issue 6, June 2017

ISSN: 2394-4404

Effects Of Elliptical Texture On Journal Bearing Characteristics Under Steady Operating Conditions And Optimization Of Dimple Depth And Area Density

Nayanjyoti Das

L. Roy

Department of Mechanical Engineering,
National Institute of Technology Silchar, Silchar, India

Abstract: ***In this present work an attempt has been made to theoretically examine the influence of elliptical texture on non-dimensional load carrying capacity, friction variable, flow coefficient of textured journal bearing. In which the performance parameters are estimated by varying the textured height, textured area density and eccentricity ratio. A non-dimensional analysis is carried out to analyze the performance characteristic of elliptical texture on journal bearing using finite difference method. The optimum value of textured depth and textured area density is obtained. The optimum parameters obtained for maximization of flow coefficient, minimization of friction variable, maximization of non-dimensional load capacity, and minimization of multi-objective function derived combining all the three individual objective functions using Genetic Algorithm. It has been found that incorporation of elliptical texture inside the bearing surface improves the friction and lubrication performance of the bearing. The results using genetic algorithm are compared with sequential quadratic programming (SQP).It is observed that textures acts as secondary reservoir which decreases the friction variable as well as increases the flow co-efficient. At an eccentricity ratio 0.9, dimple depth 0.1 and dimple area density 0.598 gives the optimum value of friction variable, flow co-efficient and non dimensional load carrying capacity.***

Keywords: hydrodynamic journal bearings, elliptical texture, lubrication, optimum value

NOTATION

R	radius of journal (m)
D	diameter of the bearing (m)
L	length of bearing (m)
C	radial clearance (m)
O	center of bearing bush
O'	center of shaft about which it rotates
e,ε	eccentricity (m), eccentricity ratio $\varepsilon = e/C$
N	journal rotation speed (rpm)
ω	Journal angular speed (rad/s)
U	linear speed of moving surface (m/s)
W	load carrying capacity of bearing or applied load at the shaft
ϕ	Attitude angle (rad)
h,$\bar{h}$	lubricant film thickness (m), non-dimensional film thickness $\bar{h} = h/C$
$\theta, \bar{y}, \bar{z}$	Non-dimensional coordinates, x/R, y/h and z/L/2, measured from the top of bearing and at the mid-plane of groove
τ_x, τ_z	Shear stress along circumferential and axial direction (N/m^2)
F	friction force due to the viscosity of lubricant (N)
W_r, W_t	load carrying components along line of centres and perpendicular to the line of centers (N)
$\bar{W}$	Non-dimensional non dimensional load

$$\text{carrying capacity} = \frac{WC^2}{6\eta UR^2L}$$

μ Coefficient of friction

$\bar{\mu}$ Friction variable = $\left(\frac{R}{C}\right)\mu$

S Sommerfeld number = $\frac{\eta N}{P}\left(\frac{R}{C}\right)^2$

I. INTRODUCTION

Hydrodynamic journal bearings are machine elements used since the beginning of the industrial revolution for the support of rotating shafts. It is used in turbo machinery, vehicles, and power plants. In general all mechanical systems with rotating shafts subjected to high surface speeds and/or applied loads. The purpose of bearing is to support a load. Deflection of the journal within the bearing can adversely affect the load carrying ability of the bearing. This deflection can be greatly reduced by increasing the diameter of the journal and decreasing its length. Now days the human beings are very much concerned about the energy saving by reducing the failure of the component with lower initial cost. The friction between the machine components produces wear and heat is generated due to which energy is losses. The success of modern journal bearings is due to the understanding that lubrication, the function of which is to separate the surfaces, is an integral part of journal bearing design. A journal bearing may be subject to Hydrodynamic, hydrostatic, boundary film lubrication. However, only hydrodynamic and boundary lubrication will be considered utilizing either liquid or gas lubricant. The primary function of lubricant is to separate surfaces, reduce friction and absorb heat. Secondary responsibilities include regulating temperature, flushing contaminants, and controlling corrosion. With introduction to the surface texture on bearing surface improves the lubricating properties. Surface texture is well defined micro dimples in different form on bearing which improves the different properties of bearing. Surface texturing technology is a newly explored technology in tribology community. It is a method of improving the friction and lubrication performance of various mechanical components. The concept of surface texturing first developed in 1990 using laser technology. After that many techniques namely Photolithography techniques, etching, Novel dressing technique, Mechanical indentation is introduced for surface texturing.

Etsion [1] observe that the improvement of load carrying capacity, friction coefficient and wear resistance of the tribological component can be improved by micro-surface texture in form of micro dimple on their surface by the help of Laser surface texturing and reviewed the current effort being made worldwide on surface texturing in general and on laser surface texturing (LST) in particular and describes some fundamental on-going research around the world with LST and describes LST is starting to gain more and more attention in the Tribology community. Priest and Taylor [2] demonstrated the technology of surface texturing is expected to be important component in future structure design.Tala-Ighil et al. [3] used finite difference numerical model to study the effect of surface textures on the lubrication of a journal bearing system under steady state condition. The geometry and the size of textures affect load capacity and friction torque. They have done analysis on three different types of texture shapes viz spherical, cylindrical and parallelepipedic. The numerical analysis indicates that texture affects important bearing characteristic. The result analysis shows that texture has more influence on the characteristics of the bearing.The effect of micro-dimples on the frictional properties is verified by Wakuda [4]. Pin-on-disk tests modelling the contact between cylindrical and planar faces were carried out for a variety of surface morphologies in which dimples were pattern machined with different size, density and geometry. Compared to a lapped smooth surface without texturing, some samples successfully realized reductions in friction coefficient from 0.12 to 0.10.Sinanoglu [5] investigated the effects of shaft surface texture on journal bearing pressure distribution. Here experimental and neural network applications were employed for analysing pressure variations on bearing system considering smooth and textured surface. With changing the density and diameter of dimples on the load bearing surfaces had a significant effect in reduction of friction was showed by Uehara et al [6]. With the determination of dimple diameter and distribution density which resulted in the minimization of friction has been obtained in this paper along with it was also shown that certain sliding velocities would produce a negative effect due to mechanisms such as side leakage. Surface texturing also improved the load carrying capacity of a journal bearing. The bearing load carrying capacity improved by micro-hydrodynamic wedge effect during conditions that pertain to hydrodynamic regime of lubrication was showed by Sinanoglu [7]. Professor John Holland of the University of Michigan envisaged the concept of these non-traditional Algorithms in the mid-sixties. Thereafter, a number of his students and other researchers have contributed to developing this field. To date of the GA studies are available through a few books(Goldberg,1989[13]). As a result of growing pace of applications, research into structural optimization is increasingly driven by real life problems. Rowe and Koshal[8]reported a new technique for optimizing hybrid journal bearings. The method involves the comparison of the bearings to be optimized with a reference bearing on the basis of load/total power, load/pumping power and load/flow. Sherbiny, Salem and Hefnawy [9] formulated optimization problem to maximize the load-carrying capacity of hydrostatic journal bearings. Optimization process is based on the well-known Rosenbrock method and from results concludes that precision bearings with small clearances and low pressure ratios are recommended for applications involving low supply pressures, while bearings with large clearances and pressure ratios close to 0.5 are recommended for applications involving high supply pressures. Hashimoto [10] has optimized the design procedure of high-speed, short journal bearings under laminar and turbulent flow conditions developed based on Successive Quadratic Programming, Genetic Algorithm and Direct Search method. Short bearing assumption to the modified turbulent Reynolds equation, simplified closed form design formulae are obtained for the eccentricity ratio, friction force, film temperature rise, supply lubricant quantity and whirl onset velocity as a function of design variables such as radial clearance, slenderness ratio and averaged viscosity of

lubricants. Design variables, which optimize the objective function given by a linear summation of temperature rise and supply lubricant quantity with respective weighting factor, are determined for a wide range of journal rotational speeds under various constraints. Bo-Suk Yang and Choi.B[11] have used enhanced artificial life algorithm for the optimum design of short journal bearings. The optimized results were compared with those of genetic algorithm and successive quadratic programming. All the results have the same tendency. The artificial life algorithm only uses the function value and doesn't need derivatives calculated analytically or numerically and so it has a strong possibility for being used for other optimization problems. Boedo and Eshkabilov[12] this paper describes an implementation of a genetic algorithm scheme suitable to the optimal shape of finite iso-viscous suitable to the optimal shape design of finite-width, iso-viscous, fluid film journal bearings under steady load carrying and steady journal rotation. Optimal bearing geometry is found to offer a small improvement in non-dimensional load carrying capacity and a substantial improvement in oil flow over purely cylindrical designs. John McCall [13] has presented Genetic algorithms (GAs) a heuristic search and optimization technique inspired by natural evolution. They have been successfully applied to a wide range of real-world problems of significant complexity. Hirani andSuh[14]describe the optimum design methodology for improving operating characteristics of fluid-film steadily loaded journal bearings. This methodology consists of (1) a simplified closed form solution to accelerate the computation, (2) finite difference mass conserving algorithm for accurate prediction of lubricant flow and power loss, (3) Pareto optimal concept to avoid subjective decision on priority of objective functions, (4) a genetic algorithm to deal with multimodal nature of hydrodynamic-bearing and develop a Pareto optimal front, (5) fitness sharing to maintain genetic diversity of the population used in genetic algorithm, and (6) axiomatic design to provide inside of objective functions and design variables. In the optimum design of journal bearings, the design variables such as radial clearance, length to diameter ratio, groove geometry, oil viscosity and supply pressure are used to simultaneously minimize oil flow and power loss. A step-by-step procedure, graphs and tables are presented to demonstrate the concept and effectiveness of suggested design methodology. The Reynolds equation is solved numerically in a finite difference grid satisfying the appropriate boundary conditions. Determination of optimum performance is based on maximization of non-dimensional load, flow coefficient, and minimization of friction variable using genetic algorithm.

II. THEORY

For steadily loaded journal bearing the non-dimensional form of Reynolds Equation is

$$\frac{\partial}{\partial\theta}\left(\bar{h}^3\frac{\partial\bar{p}}{\partial\theta}\right)+\left(\frac{D}{L}\right)^2\frac{\partial}{\partial z}\left(\bar{h}^3\frac{\partial\bar{p}}{\partial z}\right)=\frac{\partial\bar{h}}{\partial\theta} \quad (1)$$

For single axial groove journal bearing, the non-dimensional load carrying components along the line of centres and its perpendicular direction are found out from: $\bar{W}_x=\int_o^{2\pi}\bar{p}cos\theta.d\theta$ (2)

$$\bar{W}_z=\int_o^{2\pi}\bar{p}sin\theta.d\theta \quad (3)$$

Therefore the non-dimensional load carrying and attitude angle are

$$\bar{W}=\sqrt{\left(\bar{W}_x{}^2+\bar{W}_z{}^2\right)} \quad (4)$$

$$\phi=\tan^{-1}\left(\frac{\bar{W}_z}{\bar{W}_x}\right) \quad (5)$$

The bearing end flow is calculated from:

The flow rate in the dimensionless form can be written as:

$\bar{Z}=\frac{z}{L/2}, \bar{h}=\frac{h}{c}$, θ = x/R and $\bar{p}=\frac{pc^2}{6\eta uR}$

flow rate in the dimensionless form can be written as

$$\bar{q}_z=\frac{1}{2}\left(\frac{D}{L}\right)^2\int_0^{2\pi}\bar{h}^3\frac{\partial p}{\partial z}\partial\theta \quad (6)$$

Friction force can be found from:

$$F=2\int_0^{\frac{L}{2}}\int_0^{2\pi}\tau_x R d\theta dz \quad (7)$$

This can be written as:

$$\bar{F}=\frac{FC}{\eta URL}=\frac{1}{6}\int_0^{2\pi}\left(3\bar{h}\frac{\partial\bar{p}}{\partial\theta}+\frac{1}{\bar{h}}\right)d\theta \quad (8)$$

The friction variable is given by:

$$\bar{\mu}=\left(\frac{R}{C}\right)\mu=\frac{\bar{F}}{\bar{W}}=\frac{1}{6\bar{W}}\int_0^{2\pi}\left(3\bar{h}\frac{\partial\bar{p}}{\partial\theta}+\frac{1}{\bar{h}}\right)d\theta \quad (9)$$

Sommerfeld Number

$$S=\frac{\eta N}{P}\left(\frac{R}{C}\right)^2 \text{ where} P=\frac{W}{2LR} \quad (10)$$

OPTIMIZATION TECHNIQUE

Generally textures are used to serve as channels to supply lubricant to a surface of the bearing, and it is found that the height of the texture have influence in flow rate ($\bar{q}_z$), frictional variable ($\bar{\mu}$), non dimensional load carrying capacity ($\bar{W}$). In finding out optimum results using Genetic Algorithm (GA), variables called genes will form chromosome. A set of chromosome is called population. With uniform probability distribution all chromosomes in the population are initialized. The population of each generation will have feasible design variables (Chromosome) in terms of their allowable ranges but may be infeasible otherwise. The main steps involved in the genetic algorithm are discussed below and shown in a flow chart (Fig. 4.3). The generic algorithm convergence rate to true optima depends on the probability of crossover and mutation on one hand, and the maximum generation, on the other hand. In order to preserve a few very good strings, and rejecting low-fitness strings, a high crossover probability is preferred. The mutation operator helps to retain the diversity in the population, but disrupts the progress towards a converged population and interferes with beneficial action of the selection and crossover. Therefore, a low probability, 0.001–0.1, is preferred. The genetic algorithm updates its population on every generation, with a guarantee of better or equivalent fitness strings. For well-behaved functions, 30–40 generations are sufficient. For steep and irregular functions, 50–100 generations are preferred. Considering these factors, a population size of 50, mutation probability of 0.1 and a cross over probability of 0.8 have been selected. The difference between GAs and many traditional optimization methods is that GAs work with a population of points instead of a single point. On the other hand, since GAs require only function values at various discrete points, a discrete or discontinuous

function can be handled with no extra burden. This allows GAs to be applied to a wide variety of problems. Another advantage with a population-based search algorithm is that multiple optimal solutions can be captured in the population easily, thereby reducing the effort to use the same algorithm many times. Genetic algorithms perform a multiple directional search by maintaining a population of potential solutions. The population-to-population approach attempts to make the search escape from local optima GAs is very helpful when the developer does not have precise domain expertise, because GAs possesses the ability to explore and learn from their domain.

Genetic Algorithm (GA) is one of the most popular stochastical method used to find the optimum solution for all kind of problem. Since it is multi-directional search method it always ensures a global optimum solution even the computational time is very high compared with the other optimization method.

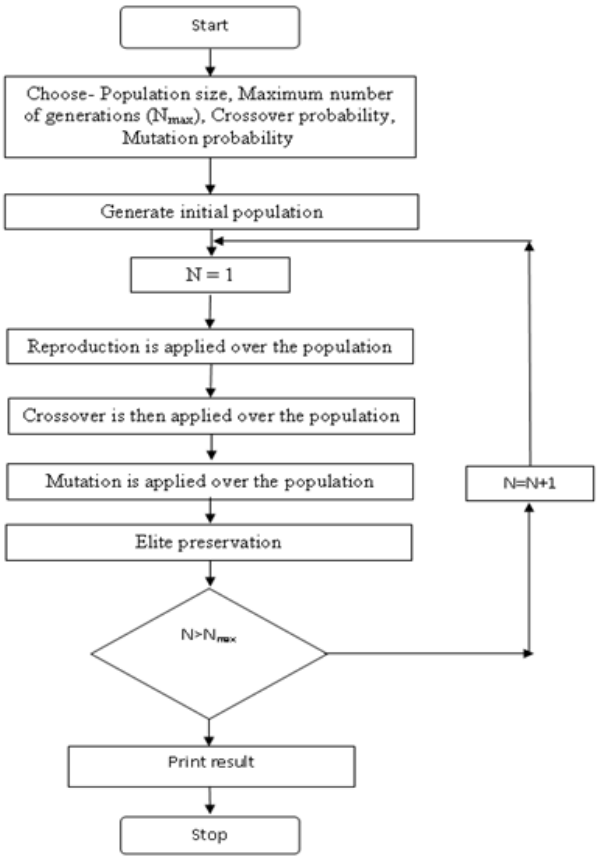

Figure 1: Flow chart for real coded Genetic Algorithm

Genetic algorithms belong to the larger class of Evolutionary Algorithms (EA), which generate solutions to optimization problems using techniques inspired by natural evolution, such as selection, crossover, mutation and inheritance. Real coded GA is capable of handling real numbers where GA is working basically on binary numbers. The genetic algorithm (GA) for optimization starts from an initial set of solutions called chromosome. In this problem two variables called genes will form chromosome. A set of chromosome is called population. With uniform probability distribution all chromosomes in the population are initialized. The population of each generation will have feasible design variables in terms of their allowable ranges but may be Infeasible otherwise. The main steps involved in the genetic algorithm are discussed below and shown in flow chart (fig.1)

Real coded GA comprises of mainly six steps:

Step 1: There are mainly four user defined parameters in the program, population size, maximum number of generation, cross over probability and mutation probability. From the trail run the best value of population size and generation size is obtained as 40 and 100 respectively. It is found that the program is converging very fast with these values. Cross over probability and mutation probability are more sensitive parameters for this program.

Step 2: In this program a population size of 50 is used. Second stage of program is to initialize the population size. So 50 chromosomes where initialize using random probability for each variable span.

Step 3: The selection operator involves randomly choosing members of the population to enter a mating pool. The operator is carefully formulated to ensure that better members of the population (with higher fitness) have a greater probability of being selected for mating, but that worse members of the population still have a small probability of being selected. Having some probability of choosing worse members is important to ensure that the search process is global and does not simply converge to the nearest local optimum. Selection is one of the important aspects of the GA process, and there are several ways for the selection.

Step 4: In GA recombination is carried out through crossover and mutation operation. The crossover operator is a method for sharing information between chromosomes. It ensures that the probability of reaching any point in the search space is never zero. The crossover operator is the main search operator in the GA. The search power of a crossover operator is defined as a measure of how flexible the operator is to create an arbitrary point in the search space. Crossover is useful in problems where building block exchange is necessary. It is suggested that GAs may work well with large crossover probability and with a small mutation probability. A single point crossover preserves the structure of the parent string to the maximum. From a set of crossover operator, linear, blended cross over and simulated binary crossover operators, it is found from trial run the simulated binary crossover gives better convergence in limited time.

Step 5: From biology view, mutation is any change of DNA material that can be reproduced. From computer science view, mutation is a genetic operator that follows crossover operator. It usually acts on only one individual chosen based on a probability or fitness function. One or more genetic components of the individual are scanned. And this component is modified based on some user-definable probability or condition. Without mutation, offspring chromosomes would be limited to only the genes available within the initial population. Mutation should be able to introduce new genetic material as well as modify existing one. With these new gene values, the genetic algorithm may be able to arrive at better solution than was previously possible. Mutation operator prevents premature convergence to local optima by randomly sampling new points in the search space. There are many types of mutation and these types depend on the representation itself. Random mutation finds a better suitability with the existing problem.

Step6: Elite preservation forms a new population from initial population and mutated one. This operator is responsible for convergence of the fitness by allowing better value to pass to the next generation.

The problem is framed with three objectives. The variables used in these problems are (two chromosomes) eccentricity ratio (Ɛ) and dimple height (r_y), and other case the two chromosomes are eccentricity ratio (Ɛ) and dimple area density (s_p). The objectives are minimization of friction variable($\bar{\mu}$), Equation 9, maximization of non-dimensional load capacity ($\bar{W}$), Equation 4, maximization of flow coefficient ($\bar{q}_z$) Equation 6. Objective

III. RESULTS AND DISCUSSION

Function framing is the same for both the cases and variable bounds are shown in Table 1 and Table 2.

Case	Variables	Lower bound	Upper bound
	Dimple height (r_y)	0	0.1
II	Dimple height (r_y)	0	0.1

Table 1: Variable bounds for the bearing problem for Dimple depth (r_y)

Case	Variables	Lower bound	Upper bound
I	Eccentricity ratio (Ɛ)	0.1	0.9
	Dimple area density (S_p)	0	0.6
II	Dimple area density (S_p)	0	0.6

Table 2: Variable bounds for the bearing problem for Dimple area density (S_p)

Formulation of Multi objective function:

Objective 1: minimization of the frictional variable of the elliptical texture bearing

Objective 2: maximization of the flow co-efficient of elliptical texture bearing

Objective 3: maximization of the non-dimensional load carrying capacity of elliptical texture bearing

Weighted sum method is used to handle three objectives at a time. Three different weightages w_1,w_2 and w_3 are considered for objective 1, objective 2 and objective 3 respectively.

$$F=w_1 \times \frac{\bar{\mu}}{(\bar{\mu}_{max}-\bar{\mu}_{min})}+w_2\left[1-\frac{\bar{q}_z}{(\bar{q}_{z_{max}}-\bar{q}_{z_{min}})}\right]+w_3\left[1-\frac{\bar{w}}{(\bar{w}_{max}-\bar{w}_{min})}\right] \quad (11)$$

Validation of the result for the textured journal bearing for length to diameter ratio (L/D=1) and the eccentricity ratio Ɛ=0.1 are given in the table 3, the dimensional value are almost same as given in [15] and small validation of the present result has been seen when compared with[15]

Characteristics	Elliptical textured bearing	[15]
Load capacity (W)	12707 N	12600 N
Sommerfeld Number (S)	0.1199	0.1210
Eccentricity Ratio (Ɛ)	0.600	0.601
Attitude Angle (ϕ)	50.531	50.4

Table 3: Validation of result for textured journal bearing [15]

In table 3 it has been shown that value for load carrying capacity for elliptical texture bearing Comes out to be 12707 N for eccentricity ratio 0.6, considering texture depth (r_y) 0.01 and texture density (S_p) 0.5 , a very less difference is observed in the attitude angle and Sommerfeld number.

Height (r_y)	Sommerfeld No(S)	Load capacity (W)	Friction Variable($\bar{\mu}$)	Flow co-efficient ($\bar{q}_z$)
0.01	1.32	0.0402	26.22	0.1586
0.02	1.30	0.0407	25.89	0.1638
0.03	1.29	0.0413	25.55	0.1692
0.04	1.27	0.0418	25.20	0.1748
0.05	1.25	0.0424	24.85	0.1807
0.06	1.23	0.0430	24.49	0.1869
0.07	1.21	0.0437	24.14	0.1934
0.08	1.20	0.0443	23.78	0.2001
0.09	1.18	0.0450	23.41	0.2072

Table 4: Steady state parameter for elliptical texture bearing for L/D=1 and eccentricity ratio (Ɛ) = 0.1

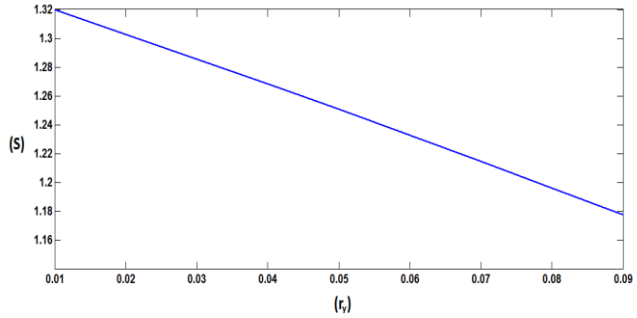

Figure 2: Variation of Sommerfeld number (S) with texture depth (r_y) for L/D=1 and eccentricity ratio (Ɛ) = 0.1

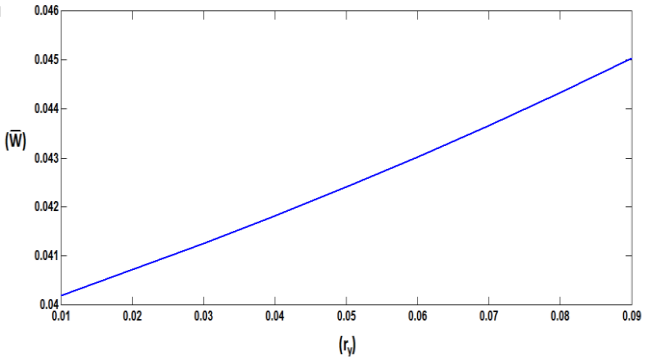

Figure 3: Variation of Non-dimensional load ($\bar{W}$) with texture depth (r_y) for L/D=1 and eccentricity ratio (Ɛ) = 0.1

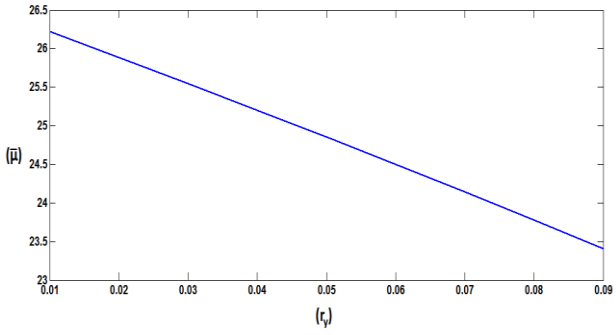

Figure 4: Variation of friction variable ($\bar{\mu}$) with texture depth (r_y) for L/D=1 and eccentricity ratio (Ɛ) = 0.1

ISSN: 2394-4404

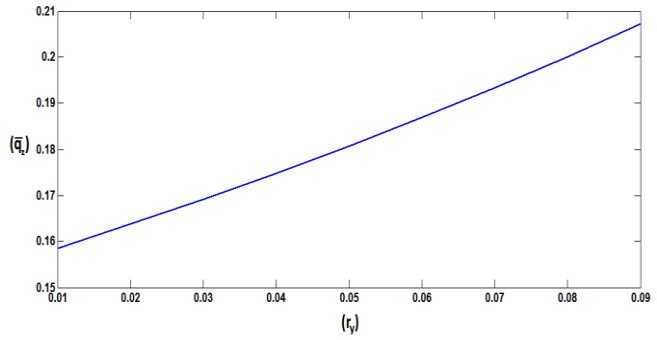

Figure 5: Variation of flow co-efficient ($\bar{q}_z$) with texture depth (r_y) for L/D=1 and eccentricity ratio (Ɛ) = 0.1

From fig.2 it has been found that the Sommerfeld number of elliptical bearing decreases with the increase in texture depth. It means that lower the value of the Sommerfeld number higher will be the load carrying capacity, so the load carrying capacity will increase with the increase in the texture depth as shown in fig.3 it is because the texture provide the more surface area to increase the non-dimensional load carrying capacity.The friction variable of elliptical textured journal bearing decreases with increase in texture depth it has been found from fig.4, it means that higher the value of texture depth more will be the friction variable. It happens because of texture act as secondary reservoir which provides more lubricant between the sliding surfaces.In fig.5 the flow co-efficient of elliptical textured increases with increase in textured depth. It has been found that because textured provide more hydrodynamic effect inside the bearing.

The obtained results from (GA) have been compared with the results obtained using sequential quadratic programming (SQP). The optimum value of fitness function obtained corresponding to minimization of friction variable has been tabulated for both GA and SQP in Table 5 for result dimple depth (r_y) and Table 6 for result dimple area density (S_p)

Eccentricity ratio(Ɛ)	GA results	SQP results
0.1	23.0337	23.0337
0.2	11.1371	11.1371
0.3	7.0788	7.0788
0.4	4.9801	4.9801
0.5	3.6642	3.6642
0.6	2.7356	2.7356
0.7	2.0234	2.0234
0.8	1.4323	1.4323
0.9	0.8871	0.8871

Table 5: Comparison of GA and SQP results for dimple depth (r_y)

Eccentricity ratio(Ɛ)	GA results	SQP results
0.1	26.0869	26.0869
0.2	12.6718	12.6718
0.3	8.0942	8.0942
0.4	5.7179	5.7179
0.5	4.2251	4.2251
0.6	3.1680	3.1680
0.7	2.3479	2.3479
0.8	1.6467	1.6467
0.9	0.9710	0.9710

Table 6: Comparison of GA and SQP results for dimple area density (S_p)

Similarly maximum load, maximum flow values are also found to match both methods. It has been observed as stated above that the results using both methods are found to be same.

The upper bound and lower bound of two variables eccentricity ratio and Dimple depth is shown in the Table 7

Variable	Lower bound	Upper bound
Eccentricity ratio (Ɛ)	0.1	0.9
Dimple depth (r_y)	0	0.1

Table 7: Variable bounds

It has been shown in the previous section that various steady state parameters like non-dimensional load capacity ($\bar{W}$), flow coefficient ($\bar{q}_Z$), and frictional variable ($\bar{\mu}$), changes with the change of dimple depth (r_y). In view of this, an attempt has been made to determine the optimum performances in terms of the three parameters mentioned above.

If the two variables namely eccentricity ratio (Ɛ) and dimple depth (r_y) are taken as chromosome (Case-I) in Table 7. The optimum results obtained for friction, flow and load is shown on Table 8.

Objective function	Optimum value	Eccentricity ratio(Ɛ)	Dimple depth(r_y)
Minimization of friction variable	0.8871	0.9	0.1
Maximization of flow co-efficient	0.3391	0.899	0.1
Maximization of load carrying capacity	0.2197	0.9	0.1

Table 8: Optimum value considering eccentricity ratio and dimple depth as chromosomes

The optimum results obtained for friction, flow and load is shown in Figures 6, 7 and 8. The figures include plots of best fitness as well as mean fitness. Genetic algorithm works on a population of individuals. So, mean is the mean fitness for the entire population at a particular iteration.

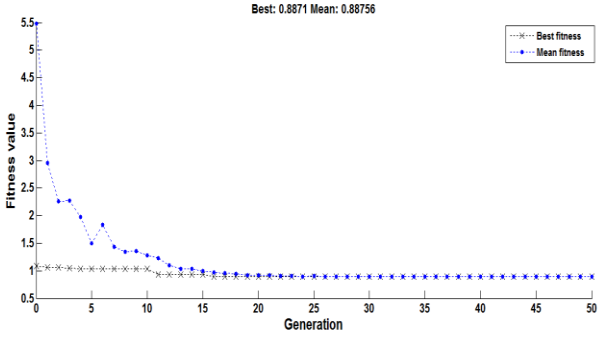

Figure 6: Fitness value considering friction variable as objective function

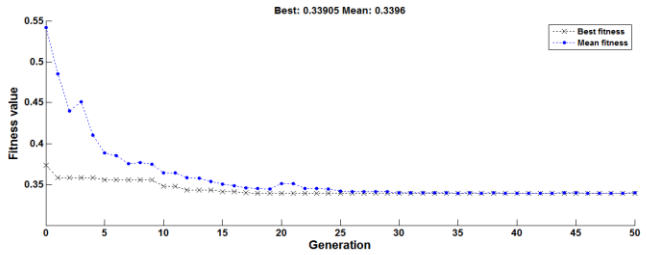

Figure 7: Fitness value considering flow co-efficient as objective function

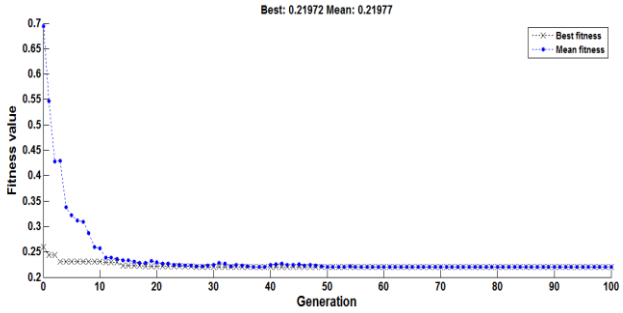

Figure 8: Fitness value considering load carrying capacity as objective function

For one variable

Variable	Lower bound	Upper bound
Eccentricity ratio (Ɛ)	0.1	0.9

Table 9: Variable bounds

In Table 10 the optimum values of friction and respective dimple height is tabulated considering eccentricity ratio as a variable.

Eccentricity ratio(Ɛ)	Optimum friction value	Dimple depth (r_y)
0.1	23.0337	0.1
0.2	11.1371	0.1
0.3	7.0788	0.1
0.4	4.9801	0.1
0.5	3.6642	0.1
0.6	2.7356	0.1
0.7	2.0234	0.1
0.8	1.4323	0.1
0.9	0.8871	0.1

Table 10: Optimum value of friction variable considering one chromosome

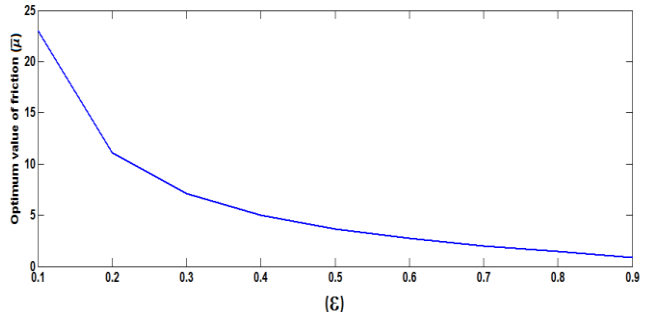

Figure 9: Variation of friction variable at optimum dimple depth for different eccentricity ratio

In Table 11 the optimum values of flow and respective dimple height is tabulated considering eccentricity ratio as a variable.

Eccentricity ratio(Ɛ)	Optimum flow value	Dimple depth (r_y)
0.1	0.8233	0.1
0.2	0.7005	0.1
0.3	0.6101	0.1
0.4	0.5404	0.1
0.5	0.4851	0.1
0.6	0.4398	0.1
0.7	0.4018	0.1
0.8	0.3689	0.1
0.9	0.3391	0.1

Table 11: Optimum value of flow co-efficient considering one chromosome

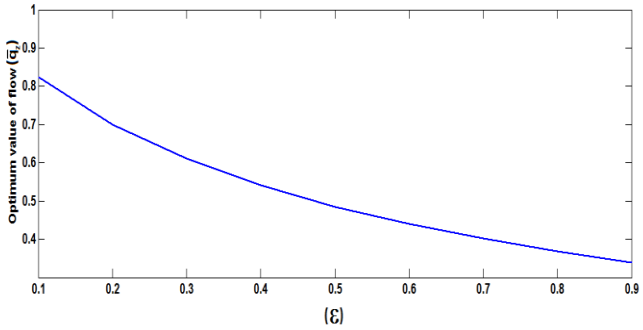

Figure 10: Variation of flow co-efficient at optimum dimple depth for different eccentricity ratio

In Table 12 the optimum values of non-dimensional load and respective dimple height is tabulated considering eccentricity ratio as a variable.

Eccentricity ratio(Ɛ)	Optimum load value	Dimple depth (r_y)
0.1	0.9562	0.1
0.2	0.9118	0.1
0.3	0.8634	0.1
0.4	0.8077	0.1
0.5	0.7405	0.1
0.6	0.6561	0.1
0.7	0.5474	0.1
0.8	0.4049	0.1
0.9	0.2197	0.1

Table 12: Optimum value of load carrying capacity considering one chromosome

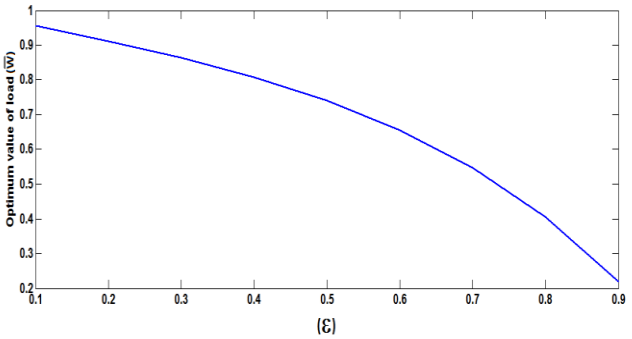

Figure 11: Variation of load carrying capacity at optimum dimple depth for different eccentricity ratio

It is clear from the Fig.9, 10 and 11 that at Ɛ=0.9 and r_y=0.1, the friction variable gives the minimum value, the

flow variable gives maximum value and load gives the maximum values, it is due to effect of texture. When texture depth increases Sommerfeld number decreases which leads to increase in load and the texture increases the lubrication so flow co-efficient also increases.

Again by combining all the objective functions at a time of the plot is shown below.The optimum values has been obtained considering minimization of the multi-objective function formed by combining all the objectives at a time as discussed in section 4.5

Eccentricity ratio(Ɛ)	Multi-objective Optimum value	Dimple depth (r_y)
0.1	1.1384	0.1000
0.2	1.0313	0.0001
0.3	1.0396	0.0001
0.4	1.0733	0.0001
0.5	1.1071	0.0001
0.6	1.1238	0.0001
0.7	1.0955	0.0001
0.8	0.9433	0.0001
0.9	0.2604	0.0001

Table 13: Optimum value of multi-objective function considering one chromosome

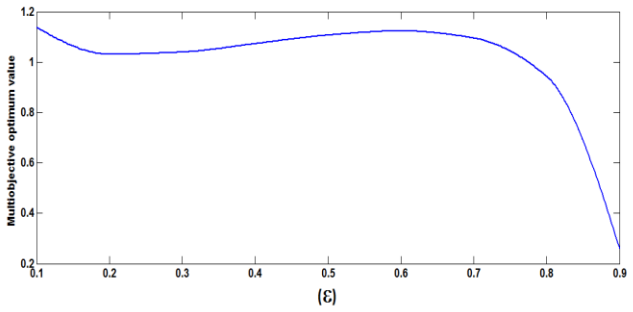

Figure 12: Variation of Multi-objective optimum value for different eccentricity ratio at optimum dimple depth

From the fig.12 it is clear that at eccentricity ratio 0.9, the multi-objective optimum value gives optimum, as the multi-objective function is minimization type. The upper bound and lower bound of two variables eccentricity ratio and Dimple area density is shown in the Table 14

Variable	Lower bound	Upper bound
Eccentricity ratio (Ɛ)	0.1	0.9
Dimple area density (S_p)	0	0.6

Table 14: Variable bounds

It has been shown in the previous section that various steady state parameters like non-dimensional load capacity ($\bar{W}$), flow coefficient ($\bar{q}_z$), frictional variable ($\bar{\mu}$), changes with the change of dimple area density (S_p). In view of this, an attempt has been made to determine the optimum performances in terms of the three parameters mentioned above.

If the two variables namely eccentricity ratio (Ɛ) and dimple area density (s_p) are taken as chromosome in Table.14. The optimum results obtained for friction, flow and load is shown on Table 15.

Objective function	Optimum value	Eccentricity ratio(Ɛ)	Dimple area density (s_p)
Minimization of friction variable	0.9710	0.9	0.598
Maximization of flow co-efficient	0.4269	0.9	0.598
Maximization of load carrying capacity	0.2429	0.9	0.598

Table 15: Optimum value considering eccentricity ratio and dimple depth as chromosomes

The optimum results obtained for friction, flow and load is shown in Figures 13, 14 and 15. The figures include plots of best fitness as well as mean fitness.

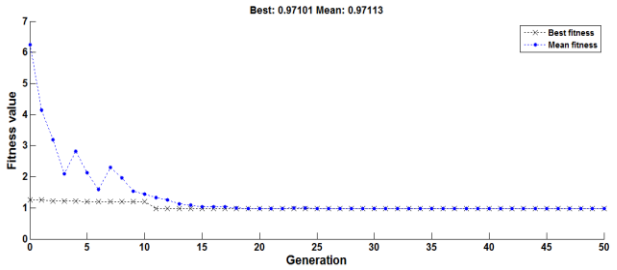

Figure 13: Fitness value considering friction variable as objective function

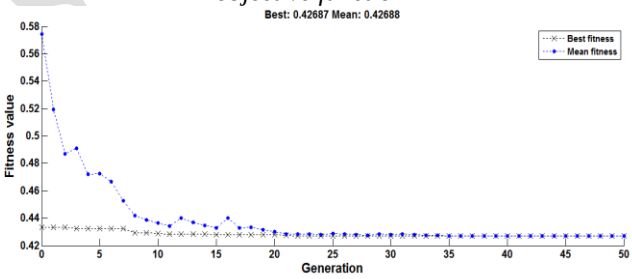

Figure 14: Fitness value considering flow co-efficient as objective function

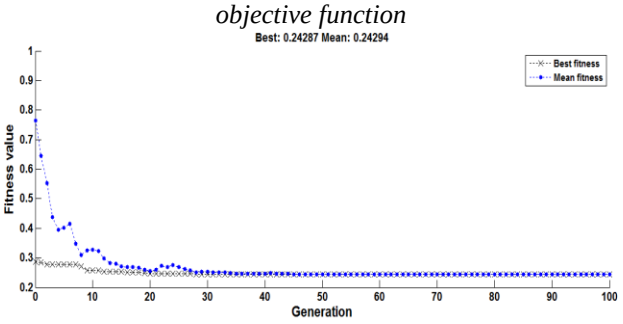

Figure 15: Fitness value considering load carrying capacity as objective function

Variable	Lower bound	Upper bound
Eccentricity ratio (Ɛ)	0.1	0.9

Table 16: Variable bounds (Case II)

In Table 17 the optimum values of friction and respective dimple area density is tabulated considering eccentricity ratio as a variable.

Eccentricity ratio(Ɛ)	Optimum friction value	Dimple area density (s_p)
0.1	26.0869	0.591
0.2	12.6718	0.591

0.3	8.0942	0.591
0.4	5.7179	0.170
0.5	4.2251	0.169
0.6	3.1680	0.167
0.7	2.3479	0.600
0.8	1.6467	0.598
0.9	0.9710	0.598

Table 17: Optimum value of friction variable considering one chromosome

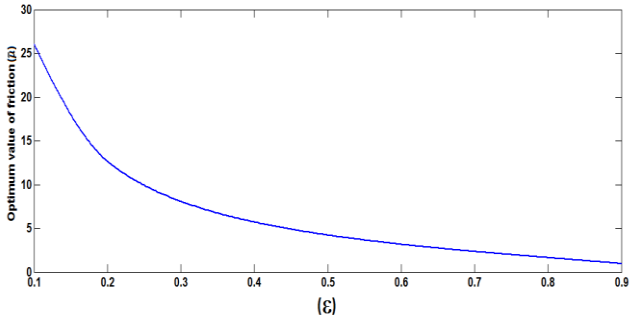

Figure 16: Variation of friction variable at optimum dimple area density for different eccentricity ratio

In Table 18 the optimum values of flow and respective dimple area density is tabulated considering eccentricity ratio as a variable.

Eccentricity ratio(Ɛ)	Optimum flow value	Dimple area density (s_p)
0.1	0.8626	0.505
0.2	0.7598	0.505
0.3	0.6798	0.505
0.4	0.6159	0.591
0.5	0.5635	0.591
0.6	0.5199	0.591
0.7	0.4829	0.598
0.8	0.4517	0.598
0.9	0.4269	0.598

Table 18: Optimum value of flow co-efficient considering one chromosome

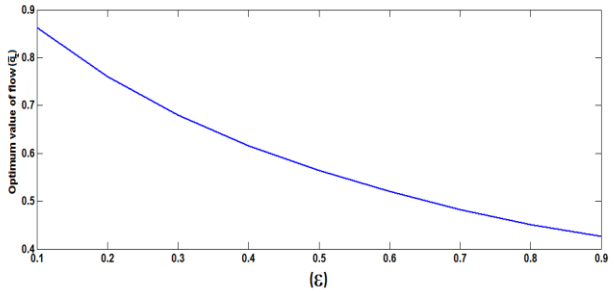

Figure 5.17 Variation of flow co-efficient at optimum dimple area density for different eccentricity ratio

In Table 19 the optimum values of load and respective dimple area density is tabulated considering eccentricity ratio as a variable.

Eccentricity ratio(Ɛ)	Optimum load value	Dimple area density (s_p)
0.1	0.9612	0.591
0.2	0.9217	0.591
0.3	0.8789	0.277
0.4	0.8287	0.167
0.5	0.7683	0.167
0.6	0.6919	0.164
0.7	0.5885	0.600
0.8	0.4458	0.598
0.9	0.2429	0.598

Table 19: Optimum value of load carrying capacity considering one chromosome

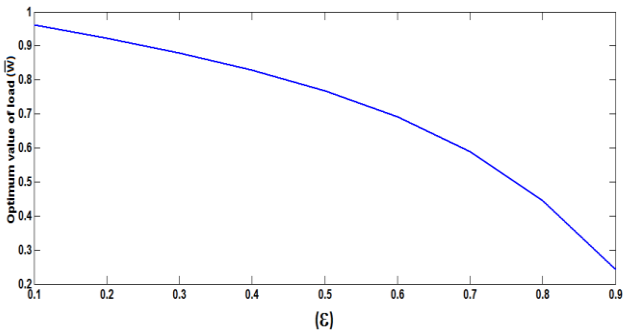

Figure 18: Variation of load carrying capacity at optimum dimple area density for different eccentricity ratio

The Fig.18, 19 and 20 shows the fitness value of friction, flow and load respectively by using Genetic algorithm. In Table 16 shows the minimization of friction, maximization of flow and load values considering eccentricity and dimple area density as the variables. It shows that in Fig.16, 17 and 18 the optimum values of friction, flow and load decreases with the increase of eccentricity ratio and at eccentricity ratio 0.9 it gives the optimum value.

The optimum values has been obtained considering minimization of the multi-objective function formed by combining all the objectives at a time as discussed above.

Eccentricity ratio(Ɛ)	Multi-objective Optimum value	Dimple area density (s_p)
0.1	1.1144	0.380
0.2	1.0349	0.181
0.3	1.0650	0.067
0.4	1.1158	0.067
0.5	1.1645	0.067
0.6	1.1946	0.067
0.7	1.1771	0.067
0.8	1.0224	0.600
0.9	0.2240	0.599

Table 20: Optimum value of multi-objective function considering one chromosome

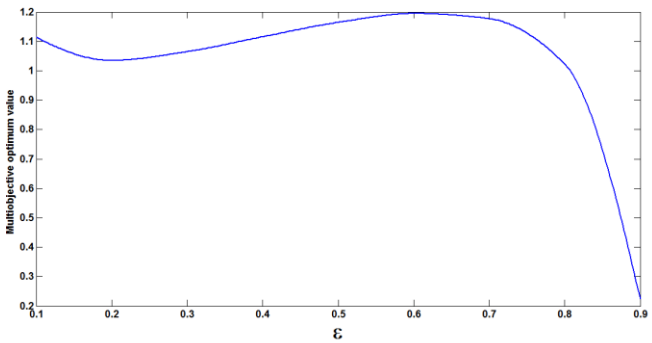

Figure 19: Variation of Multi-objective optimum value for different eccentricity ratio at optimum dimple area density

In Fig.19 the multi-objective function value along with the eccentricity is presented considering dimple area density as chromosome. It is shown from the graph that the multi-objective function value slight decreases after that it increases slight and at the last it gradually decreases with the increase of the eccentricity ratio.

IV. CONCLUSION

An improvement in performance of the bearing in terms of decrease in power loss has been found since there is decrease in friction variable. Load carrying capacity of elliptical textured bearing increases with the increase in texture depth. Flow co-efficient of elliptical textured bearing increases with the increase in texture depth. Friction variable of elliptical textured bearing decreases with the increase in texture depth.GA gives a reduction in non-dimensional friction variable with plain journal bearing. The depth location and area density to obtained this objective for elliptical textured bearing are dimple depth (r_y) = 0.1 and dimple area density (S_p) = 0.598 at Ɛ=0.9.Flow co-efficient is another important parameter in journal bearing design. So optimizing the depth and area density of elliptical textured bearing improves the non-dimensional flow rate. At dimple depth (r_y) = 0.1 and dimple area density (S_p) = 0.598 elliptical textured bearing shows high performance. For higher load carrying capacity of journal bearing, incorporation of elliptical texture at dimple depth (r_y) =0.1 and dimple area density (S_p) = 0.598 gives the better improvement.

REFERENCES

[1] Etsion, I., 2005, "State of art in Laser Surface Texturing", Journal of Tribology, 127, pp.248-253.
[2] Priest, M., Taylor, C.M., 2000, "Automobile engine Tribology approaching the surface wear", 241, pp.193-203.
[3] Tala-Ighil, N., Maspeyrot, P., Fillon, M., and Bounif, A., 2007, "Effect of surface texture on journal bearing characteristics under steady state operating", Tribology International, Vol-44, pp-211-219.
[4] Wakuda, M., Yamauchi, Y., Kanzaki, S., Yasuda, Y., 2003, "Effeect of Surface Texturing on Friction Reduction between Ceramic and Steel materials under lubricated Sliding contact wear", 254, pp.356-363.
[5] Sinanoglu, C., Nair, F., and Karamis, M.B., 2005, "Effects of shaft surface texture on journalbearing pressure distribution". Journal of Materials Processing Technology 168, pp. 344-353.
[6] Uehara,Y., Wakuda,M., Yamauchi,Y., Kanzaki,S., Sakaguchi,S.,2003, "TribologicalProperties of dimpled silicon nitride under oil lubrication", Journal of Europeanceramic society, 24(2), pp. 369-373.
[7] Sinanoglu, C., 2009, "Investigation of load carriage capacity of journal bearings by surface texturing", Industrial Lubrication and Tribology, 61(5), pp.261-270.
[8] Rowe. W., and Koshal.D.,1980, "A New Basis for the Optimization of Hybrid Journal Bearings",Wear, Vol. 64, pp. 115 – 131
[9] Sherbiny, M.E., Salem F., and Hefnawy, N.E., 1984, "Optimum Design Of Hydrostatic Journal Bearings Part I: Maximum Load Capacity", J. TribologyInternational, Vol. 17, 3, pp. 155-161.
[10] Matsumoto, K., and Hashimoto, H., 2001, "Improvement of Operating Characteristics of High-Speed Hydrodynamic Journal Bearings by Optimum Design: Part I— Formulation of Methodology and Its Application to Elliptical Bearing Design", J. Tribology, Vol.123, 2, pp. 305-313.
[11] Yang, B.S., Lee, Y.H., and Choi, B.K., and Kim, H.J., 2001, "Optimum Design of Short Journal Bearings By Artificial Life Algorithm", J. Tribology International 34, pp. 427–435.
[12] Boedo S., and Eshikabilov S., 2003, "Optimal Shape Design of Steadily Loaded Journal Bearing Using Genetic Algorithm" ASLE Trans., Vol. 46, 1, pp. 134-143.
[13] McCall, J., 2005, "Genetic Algorithms for Modeling and Optimization", Original Research Article, Journal of Computational and Applied Mathematics, Vol. 184, 1, pp. 205-222.
[14] Hirani H., and Sus N., 2005,"Journal bearing design using multiobjective genetic algorithm and axiomatic design approaches", ASLE Transactions., Vol. 38, pp. 481-491.
[15] Tala-Ighil, N., Maspeyrot, P., Fillon, M. and Bounif, A, 2007, "Effects of surface texture on journal-bearing under steady-state operating conditions", Engineering Tribology, Vol.221, pp. 623-633.